

- ⁴P. T. Coleridge, A. A. M. Croxon, G. B. Scott, and I. M. Templeton, *J. Phys.* E 4, 414 (1971); 4, 928 (1971).
- ⁵M. I. Chodorow, Ph. D. thesis (MIT, 1939) (unpublished). The potential used in the present work was obtained by interpolating the data quoted by G. A. Burdick, *Phys. Rev.* 124, 138 (1963).
- ⁶B. R. Cooper, E. L. Kreiger, and B. Segall, *Phys. Rev.* B 4, 1734 (1971).
- ⁷M. J. G. Lee, *Phys. Rev.* B 2, 250 (1970).
- ⁸P. T. Coleridge and B. R. Watts, *Can. J. Phys.* 49, 2379 (1971).
- ⁹R. E. Doezema and J. F. Koch (unpublished).
- ¹⁰D. L. Martin, *Phys. Rev.* 170, 650 (1968).
- ¹¹D. W. Osborne, H. E. Flotow, and F. Schreiner, *Rev. Sci. Instr.* 38, 159 (1967).
- ¹²F. D. Manchester, *Can. J. Phys.* 37, 909 (1959).
- ¹³M. Griffel, R. W. Vest, and J. F. Smith, *J. Chem. Phys.* 27, 1267 (1957).
- ¹⁴M. R. Halse, *Phil. Trans. Roy. Soc. London* A265, 507 (1969).
- ¹⁵R. W. Stark and S. Auluck (unpublished).
- ¹⁶G. Grimvall, *Phys. Cond. Matter* 11, 279 (1970).
- ¹⁷M. J. G. Lee and D. Nowak, *Phys. Rev. Letters* 26, 1314 (1971). Note that an equation following Eq. (9) of this paper should read $m_{\text{opt}}/m \approx 1.41$, not 1.14.
- ¹⁸D. Pines and P. Nozières, *The Theory of Quantum Liquids* (Benjamin, New York, 1966), p. 332.
- ¹⁹L. Hedin and S. Lundqvist, in *Solid State Physics*, Vol. 23, edited by H. Ehrenreich, F. Seitz, and D. Turnbull (Academic, New York, 1969), p. 102.
- ²⁰J. F. Cooke, H. L. Davis, and R. F. Wood, *Phys. Rev. Letters* 25, 28 (1970).
- ²¹M. J. G. Lee, *Phys. Rev. Letters* 26, 501 (1971).
- ²²N. E. Christensen, *Solid State Commun.* 9, 749 (1971).

Thermal and Electrical Conductivity of Pure Tin from 4.5 to 77 °K[†]

Michael C. Karamargin,* C. A. Reynolds,† F. P. Lipschultz, and P. G. Klemens

Department of Physics and Institute of Materials Science, University of Connecticut, Storrs, Connecticut 06268

(Received 3 December 1971)

The thermal and electrical conductivities of two pure single crystals of tin have been measured. The samples were oriented at 72° and 6° with respect to the tetragonal axis of tin. The thermal conductivity values for the two samples were fit to the relation $(\alpha T^n + \beta/T)^{-1}$ from 4 to 12 °K with n approximately 3.2 for both samples. This large value is attributed to dispersion in the phonon spectrum which causes an approximate 4.2-power dependence with temperature of the specific heat over the same temperature range. The electrical-resistivity value of the two pure samples was found to obey the Bloch-Grüneisen expression over a wide range with a Debye temperature of 125 °K and with a small additional residual resistivity. The anisotropy of the thermal conductivity exhibits a slight maximum at 10 °K, attributable to the relative effect of impurity scattering and an anisotropic band structure. The anisotropy of the electrical conductivities exhibits a more pronounced maximum around 20 °K because of an additional effect of area differences of Brillouin-zone segments on the Fermi surface when small-angle scattering dominates. The ratio of electrical anisotropy to thermal anisotropy at the maximum was found to be approximately 1.27, which compares well with the theoretically predicted value of 1.26 from the area differences at the zone segments in the 90° and 0° orientations.

I. INTRODUCTION

This paper reports the results of thermal and electrical-conductivity measurements on two pure single crystals of tin from 4.5 to 77 °K. These two samples had different crystallographic orientations with respect to the tetragonal axis of tin, one being nearly parallel (6°) and the other nearly perpendicular (72°). A variable-temperature cryostat consisting basically of a thermally isolated Swenson-type heat exchanger¹ cooled by circulating helium vapor was employed for the measurements. The thermal conductivity of the samples was measured by the longitudinal-heat-flow method. The temperature gradient was determined by calibrated germanium resistors. The electrical resistivity

of both samples was measured potentiometrically along the identical length as for the thermal-conductivity measurements. An evaluation of the electrical-resistivity anisotropy defined by $a_E = \rho_{(||)}/\rho_{(\perp)}$ could then be obtained from the measured resistivity of the two samples. Previous measurements on the anisotropy of the electrical resistivity for pure tin^{2,3} have indicated that a maximum occurs in the vicinity of 20 °K, and it was of interest to observe the behavior of the thermal anisotropy $a_T = \kappa_{(\perp)}/\kappa_{(||)}$ given by the ratio of thermal conductivities of the two samples. A comparison of the electrical and thermal anisotropies for two pure samples of tin above 4.2 °K has not been previously reported because of the lack of thermal-conductivity measurements on pure oriented crystals in this temperature

range.

II. EXPERIMENTAL METHOD

A. Sample Preparation

Both of the samples used in this experiment were prepared from Johnson-Matthey spectroscopically pure 99.999% tin obtained from the Jarrell Ash Company, Waltham, Massachusetts. The samples were single crystals grown by the Bridgeman technique⁴ in precision 2-mm-i. d. glass tubing. The grown crystals were removed from the Pyrex containers by immersion in a 48% solution of hydrofluoric acid. This mixture did not appear to have any effect on the tin other than removing the Pyrex. The samples were then etched in concentrated hydrochloric acid for approximately 30 sec in preparation for orienting them in an optical goniometer.⁵ Both samples were found to be single crystals over approximately 8-cm length. The orientation of the principal axes of the crystals with respect to the sample axis was found to be 72 and 6° with an accuracy of $\pm 1.5^\circ$.

B. Cryostat and Measurement

The variable-temperature cryostat that was designed and built for this experiment incorporates many of the features first utilized by Swenson and Stahl.¹ It consists basically of a thermally isolated thermal platform and heat exchanger mounted inside a larger experimental vacuum chamber. This chamber is surrounded with liquid helium with the thermal platform being cooled by a steady flow of helium vapor through the exchanger. The experimental samples are suspended in vacuum from this platform, with one end being held at the platform temperature and the other end heated above it to produce a temperature gradient along the sample. The thermally isolated heat exchanger consists of a 190-cm length of $\frac{1}{8}$ -in. -o. d. $\frac{1}{16}$ -in. -i. d. copper tubing that is wound around a short section of copper pipe. Temperature control is provided by a standard regulating circuit that controls the current to a heater wound over the tubing.

An essential feature of this cryostat is that the total heat content of the evaporating helium gas is utilized in addition to the latent heat of vaporization. The cooling of the thermal platform is thereby made a more efficient process, with only a few liters of liquid helium being required to span the range from 4 to 77°K. The temperature stability of the cryostat is found to be approximately 0.04% at temperatures below 10°K and 0.08% at temperatures above 60°K.

All temperature gradients were determined by monitoring the electrical resistance of two Cryocal Inc. germanium resistors that were calibrated ac-

ording to the manufacturer's specifications. These resistors were attached to small copper clips that also served as potential probes during the measurement of electrical resistance. Once placed on a sample, these clips were not disturbed until all thermal- and electrical-conductivity measurements were completed. This procedure minimizes any geometrical error associated with relating the two sets of data. However, separate low-temperature runs were required for the thermal- and electrical-resistivity measurements, since the latter required the placement of a low-resistance copper wire to the sample end. This wire carried the measuring current. At each temperature at least six or seven different values of the current were used, and the resistance was determined potentiometrically as described previously.⁶ The probable error of the electrical resistance is found to be never more than 0.6% above 35°K, but the error increases to approximately 3% at 15°K. This rather large error results from the very small value of the resistance of pure tin at these temperatures and from a current limit of $\frac{1}{2}$ A in the current leads, since all of the resistivity measurements were made in a vacuum.

Upon completion of the electrical-resistivity data, the system was allowed to warm up, the cryostat was opened, and the copper-resistivity current leads removed from each sample. Thermal-conductivity measurements were then made in a similar manner, with the thermal platform held at the desired temperature by the regulating system. Several heater-power settings were employed at each platform temperature with the data being corrected for stray heat losses resulting from the wiring connections on the warm end of the sample. Corrections were also made for the heat generated in the leads carrying current to the sample heaters.

The heaters themselves consist of small copper spools over which 70 ft of 0.0025-in. Evanohm wire is wound noninductively. This wire provides a resistance on the order of 9000 Ω , constant to within 0.1% at all temperatures from 4.2 to 75°K. Heat losses due to radiation were minimized by enclosing the entire sample with a copper-foil radiation shield that was held at the temperature of the thermal platform. At the higher temperatures (above 60°K) a small radiation correction was made. This correction never exceeds 1% of the heater power at worst. The probable error in the thermal conductivity results essentially from a fixed geometrical factor and a calibration error associated with the uncertainty in the true temperature. The latter increases with temperature, as specified by Cryocal Inc., and results in a total probable error in the thermal conductivity of the order of 1.0% at temperatures above 40°K. At

lower temperatures the probable error is smaller; below 20 °K it is of the order of 0.5%.

III. EXPERIMENTAL RESULTS AND ANALYSIS

A. Thermal Conductivity

The two pure-tin samples were designated P-1 and P-3. Sample P-1 had its cylindrical specimen axis inclined 6° with respect to the tetragonal axis of the tin crystal, whereas the orientation of P-3 was at an angle of 72°. Both samples were optically found to be single crystals over lengths approximately 10 and 8 cm, respectively. The thermal conductivity was obtained by the longitudinal-heat-flow method: If a measured rate of heat flow \dot{Q} is established along a specimen of cross-sectional area A with a temperature difference ΔT over a length L , the thermal conductivity κ is given by

$$\kappa = \dot{Q}L / (A\Delta T). \quad (1)$$

The values of the thermal conductivity thus measured on the two specimens are shown in Fig. 1.

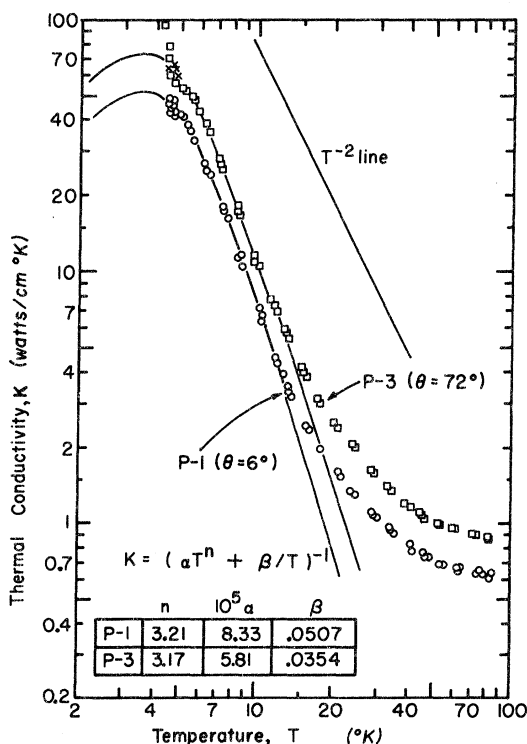


FIG. 1. Total thermal conductivity of the two pure samples. Measured values are shown by the circles for sample P-1 and squares for sample P-3. The solid lines are calculated from the relation $\kappa = (\alpha T^n + \beta/T)^{-1}$ with the values shown in the inset. The X points for P-3 at 4.5 °K were obtained by pumping on the cryostat bath and capillary. A line with slope -2 on the log-log plot is shown for comparison.

The values for P-1, oriented nearly parallel, are seen to lie significantly below those of P-3 at all temperatures by a ratio of from 1.4 to 1.5. This difference can be attributed to the anisotropic conduction properties of tin. At the lowest temperatures, the measured values agree well with those reported by previous investigators on samples of similar purity.⁷⁻⁹ At the highest temperatures, the data of P-3 approach those of Lees,¹⁰ who measured a polycrystalline specimen from 100 °K up. At the temperature of highest thermal conductivity (close to 4.2 °K), it was difficult to establish a temperature gradient along sample P-3 without excessively raising the average temperature. However, it was possible to obtain reliable data below 5 °K by pumping on both the helium bath and the heat-exchanger exhaust, thus lowering the temperature of the platform down to 3.8 °K. The application of substantial heater power then allowed data to be taken near 4.5 °K. The actual data points thus obtained for sample P-3 are shown by crosses in Fig. 1.

An initial analysis of the thermal conductivity for both samples was attempted by plotting T/κ vs T^3 for all data points below 16 °K. This assumes a relation of the form

$$\kappa = (\alpha T^2 + \beta/T)^{-1} \quad (2)$$

for the electronic thermal conductivity below $\frac{1}{10}\Theta$, where Θ is the Debye temperature. The two terms describe the thermal resistivity due to electron-phonon interactions and defect scattering, respectively. It is implied that the lattice component of the thermal conductivity can be neglected in these pure samples. The above-mentioned plot would therefore yield a straight line with slope α and intercept β at $T=0$. However, the resulting curve was not a straight line nor was it straight over two separate portions as reported by Rosenberg for cadmium and zinc.¹¹ The plot curved progressively upward, thus indicating a power dependence greater than two for the temperature dependence of the intrinsic resistivity term. A generalized least-squares analysis was made to obtain an optimum power (n) for both sample curves. Assuming the form $\kappa = (\alpha T^n + \beta/T)^{-1}$, a best fit for all the data for each sample up to 12 °K was found for values of n , α , and β . Results are given in Table I.

The resulting curves obtained from these parameters are drawn through the data points in Fig. 1 so that the quality of the fit can be judged. These calculated curves were extended below the limit of our measurements down to 2 °K. Both curves predict a maximum in thermal conductivity at approximately 3.5 °K, slightly below the superconducting transition temperature of 3.72 °K. These values agree well with those measured by other investigators⁷⁻⁹ but are still substantially below the purest

TABLE I. Values of coefficients n , α , and β in the equation $1/\kappa = \alpha T^n + \beta/T$, found by a least-squares analysis to best fit the thermal-conductivity data up to 12°K.

Sample	n	α [cm W ⁻¹ (°K) ¹⁻ⁿ]	β [cm (°K) ² W ⁻¹]
P-1	3.21	8.38×10^{-5}	5.07×10^{-2}
P-3	3.17	5.81×10^{-5}	3.54×10^{-2}

tin that has ever been measured by Zavaritskii¹² or by Guenault,¹³ where peaks on the order of 200 W/cm °K were observed at temperatures close to 1.5°K.

Equation (2) could thus be replaced by

$$\kappa = (\alpha T^{3.2} + \beta/T)^{-1}, \quad (3)$$

with the appropriate value of α and β given above for each of the two samples.

A temperature dependence greater than two is not unusual and has been obtained for many other metals.^{11,14,15} In the present case, the primary cause of this departure from a T^2 dependence may lie in the fact that the phonon spectrum departs from the Debye model, thereby leading to a departure of the lattice specific heat from a T^3 law. As a check of this fact, specific-heat data on pure tin taken from Corruccini and Gniewek¹⁶ were plotted as a function of temperature in the range 4 to 12°K. This curve is shown in Fig. 2 along with a dotted line showing a $T^{4.2}$ dependence. Because the electrons themselves introduce a specific heat proportional to T and their relaxation time varies inversely as the lattice specific heat, a 4.2-power dependence of the specific heat for phonons will result in a 3.2-power dependence of the intrinsic thermal resistivity. The agreement with this 4.2-power line and the actual data appears to be quite close over the same temperature range. This signifies that the actual number of phonons available at these temperatures is larger than one would normally expect. This particular result has been noted for tin before by Wolfram *et al.*,¹⁷ who analyzed the vibrational spectrum. That analysis found the optical and acoustic modes for the tin lattice to be strongly affected by edges of Brillouin zones. This subsequent dispersion results in a large maximum in the longitudinal acoustic branch near the center of the zone and can explain the rapid rise in the specific heat at low temperatures. At higher temperatures this effect is lost and the fit to the data by means of Eq. (3) becomes impossible. The fact that the rapid change in the specific heat coincides with the large value of n indicates that there is a strong interaction between the electrons and the transverse phonons in this temperature range. Unfortunately, departures of the thermal resistivity from a T^2 dependence cannot be explained in all cases by deviations of the specific heat from a T^3

dependence, as was pointed out by Bogaard and Gerritsen¹⁵ in the case of cadmium.

The values of the constants α and β yield the interesting result that α and β of the two specimens are approximately proportional, i. e.,

$$\alpha(\text{P-1})/\alpha(\text{P-3}) = \beta(\text{P-1})/\beta(\text{P-3}) \approx 1.47. \quad (4)$$

This fact is not unusual, but it does point out that phonon scattering and impurity scattering are equally effective in the two directions of transport and are similar in regard to their thermal resistivity. However, this may be a coincidence. The constant β is related to the residual resistivity ρ_0 by $\beta = \rho_0/L$, where L is the Lorenz constant. For pure samples, ρ_0 will be determined by trace amounts of impurities that are present. Although both samples were prepared from the same melt and were grown and handled in the same manner, their *exact* similarity with respect to trace amounts of impurities is unlikely. Furthermore, β is determined from points taken from 4.2 to 12°K, all above the maximum, so that it is not as well determined as α .

B. Electrical Resistivity

The electrical resistivity of the two pure speci-

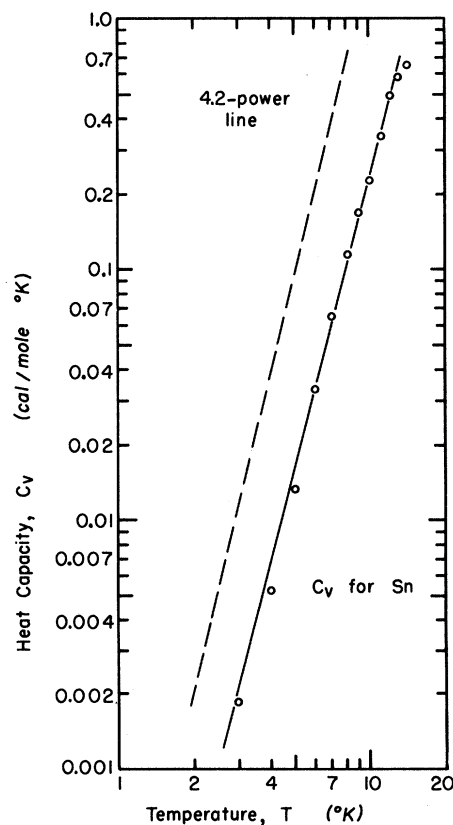


FIG. 2. Specific heat of tin from 4 to 12°K. Circles are values taken from Ref. 16. A line with slope 4.2 on the log-log plot is shown for comparison.

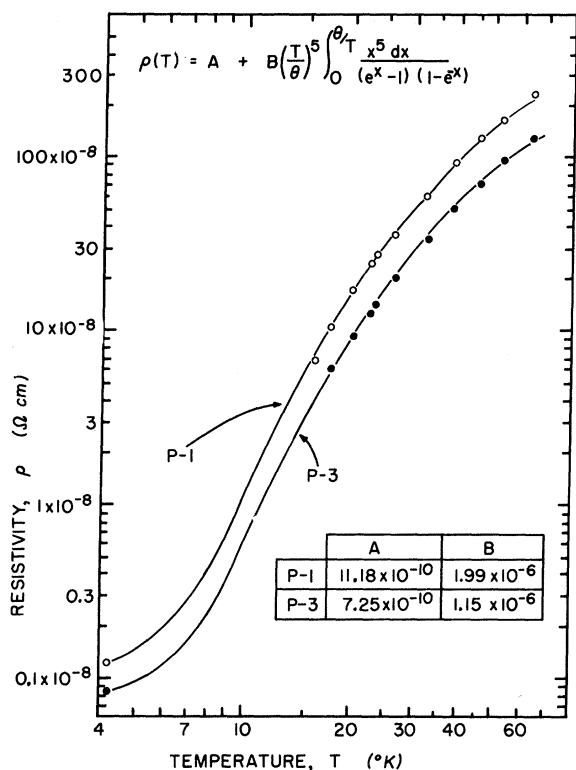


FIG. 3. Electrical resistivity of the two pure samples. Measured values are shown by the open circles for P-1 and closed circles for P-3. The solid lines are calculated from the Bloch-Grüneisen expression for the values of A and B (in Ω cm) shown in the inset and for $\Theta = 125^\circ\text{K}$.

mens was measured by the potentiometric technique during a separate run. Because the current was limited to $\frac{1}{2}$ A in the current leads on the variable-temperature cryostat, reliable resistivity data could not be obtained below 15°K . Data above this temperature up to 78°K were taken by employing the same unmoved clamps as potential taps that were used as thermometer attachments during the thermal-conductivity run. Possible spurious temperature gradients across each sample were monitored potentiometrically by the resistance of the two germanium resistors that were attached to each potential clamp. Any errors resulting from spurious thermoelectric potentials were thereby avoided; data were accepted only when no measurable thermal gradients were present. Application of currents up to $\frac{1}{3}$ A to the samples did not appear to cause any measurable heating over short periods of time.

The actual electrical-resistivity data for both samples is shown in Fig. 3. There is good agreement with results obtained for the ideal electrical resistivity of tin by other investigators who also utilized single crystals.¹⁸ Of these previous measurements, the results of Aleksandrov and D'Yakov³ appear to be the most comprehensive, since they

employed very pure single crystals of parallel and perpendicular orientations over a very wide range of temperature (3.7 – 273°K). The present results agree very well with theirs. Figure 3 also shows a theoretical fit to the experimental points using the Bloch-Grüneisen expression given in the top of the figure. The optimum values for the constants A and B as determined by computer fit are also shown in the bottom of the figure. Here, the constant A represents the residual resistance ρ_0 for the measured samples. As a check on this value of the residual impurity, a different cryostat was used to measure the resistivity of both pure samples at 4.2°K by direct immersion in a helium bath. The results are given in Table II. Currents of up to 3 A were utilized for these measurements with the potential difference being determined with a Honeywell (Model No. 2783) potentiometer.

As a check on the goniometer measurement of the orientation for both of the pure samples, the ice-point resistivity was also determined by employing the same apparatus with the samples immersed in packed ice and distilled water. The results are also in Table II.

Since the anisotropic resistivity at 273°K for pure tin is well known,^{6,19} the two resistance values given above could be utilized as a check on the orientation of the two samples as determined by the optical goniometer. The agreement was found to be good.

C. Theoretical Analysis of Electrical Resistivity

The measured electrical resistivity at 4.2°K for both samples is considerably higher than the ideal resistivity deduced by other workers,^{3,20} and it is expected that the residual resistivity would be dominant below about 8°K . At any temperature higher than 10°K the ideal resistivity should be dominant. In order to represent the temperature dependence, the total resistivity is assumed to obey the Bloch-Grüneisen relation,

$$\rho = A + B(T/\Theta)^5 \int_0^{\Theta/T} [x^5 e^x (e^x - 1)^{-2} dx], \quad (5)$$

where A represents the residual resistivity. The ideal resistivity should vary as T^5 at sufficiently low temperatures, as has indeed been found by Zernov and Sharvin.²⁰ Our measurements, save

TABLE II. Residual ($T=4.2^\circ\text{K}$) and ice-point resistivities of samples P-3 and P-1.

Sample	Temp. ($^\circ\text{K}$)	Resistivity (Ω cm)
P-3	4.2	$(8.6 \pm 0.5) \times 10^{-10}$
P-1	4.2	$(12.4 \pm 0.5) \times 10^{-10}$
P-3	273	$(9.395 \pm 0.056) \times 10^{-6}$
P-1	273	$(13.905 \pm 0.083) \times 10^{-6}$

for the 4.2 °K point, do not extend below about 15 °K, so that we are unable to test the low-temperature limiting behavior of the ideal resistivity ρ_i .

Assuming a dependence given by Eq. (5), optimum values of A and B were obtained by a least-squares fit to the data, using successive choices of Θ . A value of $\Theta = 125$ °K gave a good fit up to 60 °K for both samples; trial values of 120 and 130 °K resulted in a poorer fit.

One can also obtain a value of Θ from $\rho_i(T_1)$ at some very low temperature and $\rho_i(T_2)$ at some high temperature, using a limiting case²¹ of Eq. (5):

$$\rho_i(T_1)/\rho_i(T_2) = 497.6(T_1)^5/(\Theta^4 T_2), \quad (6)$$

where $T_2 \gg \Theta$, $T_1 \ll \Theta$. Taking 273 °K for T_2 and 4.2 °K for T_1 , and using published data,¹⁸ i. e., $\rho_i(273) = 9.40 \times 10^{-6}$ Ω cm and $\rho_i(4.2) = 1.0 \times 10^{-10}$ Ω cm, a value of $\Theta = 123$ °K is obtained.

It should be remembered, however, that Eq. (5) is based on a model of a spherical Fermi surface without zone boundaries. Since this is not a realistic model, agreement with Eq. (5) is fortuitous, and the parameter Θ in Eq. (5) or Eq. (6) should not be identified with the Debye temperature as defined by the low-temperature specific heat,¹⁶ which is around 165 °K.

IV. ANISOTROPIC PROPERTIES OF TIN

The specific anisotropic behavior of tin can be readily observed by a comparison of data for P-1 and P-3, oriented at 6° and 72°, respectively. We define the quantity a'_E to be the electrical-resistivity anisotropy and a'_T , that of the thermal-conductivity anisotropy for the orientation of the samples actually used, so that,

$$a'_E = \rho(\text{P-1})/\rho(\text{P-3}) \quad \text{or} \quad a'_T = \kappa(\text{P-3})/\kappa(\text{P-1}),$$

where ρ and κ are the measured values of the electrical resistivity and thermal conductivity, respectively. They are related to the anisotropies for ideal orientation, $a_E = \rho(0^\circ)/\rho(90^\circ)$ and $a_T = \kappa(90^\circ)/\kappa(0^\circ)$ through the following relations¹⁹:

$$\rho(\theta) = \rho(90^\circ) [1 + (a_E - 1) \cos^2 \theta],$$

$$1/\kappa(\theta) = [1/\kappa(90^\circ)] [1 + (a_T - 1) \cos^2 \theta],$$

where $\rho(\theta)$ is the electrical resistivity, and $\kappa(\theta)$ is the thermal conductivity of a sample with cylindrical axis at an angle θ with respect to the tetragonal axis of the lattice. One may use these equations to transform a'_E and a'_T to a_E and a_T , the anisotropies for ideal orientation:

$$a_E = \frac{a'_E - 1}{\cos^2 6^\circ - a'_E \cos^2 72^\circ} + 1;$$

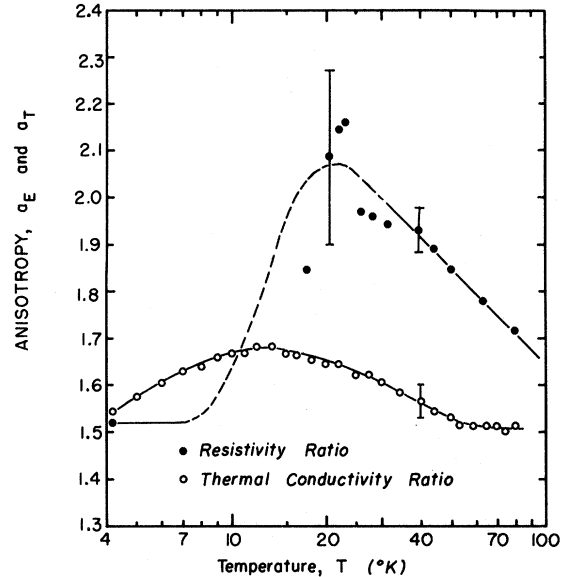


FIG. 4. Electrical-resistivity (a_E) and thermal-conductivity (a_T) anisotropies of pure tin, adjusted to sample orientations of 0° and 90°. The values of a'_E and a'_T are obtained from the data for samples P-1 and P-3, and transformed to a_E and a_T . The values of a_E are shown by the closed circles; the values of a_T are shown by the open circles.

$$a_T = \frac{a'_T - 1}{\cos^2 6^\circ - a'_T \cos^2 72^\circ} + 1.$$

The values of the anisotropies, a_E and a_T , obtained from the experimental data, and transformed to the values which would be obtained for ideal geometry, have been plotted in Fig. 4 against temperature. The open circles are the thermal-conductivity ratios and the solid points the electrical-resistivity ratios. The electrical-resistivity data are incomplete since no data were taken below 17 °K with the variable-temperature cryostat. The single point taken at 4.2 °K with the other cryostat yields a corrected resistivity ratio of 1.52 which should be valid up to about 7 °K. The probable behavior of the resistivity anisotropy between 7 and 17 °K has been indicated by the dashed line. The general form of this curve shows a maximum in the vicinity of 20 °K. Similar behavior has been observed by other investigators in tin^{2,3} and in cadmium and zinc.²² The anisotropy of the thermal conductivity exhibits a less pronounced maximum at a temperature close to 10 °K. There appears to be no other measurements of the thermal-conductivity anisotropy of tin at intermediate temperatures.

The probable error in a_E for both curves is shown by the error bars close to 40 °K and also near 20 °K. At the latter temperature there is significant scatter since each single measured resis-

tivity value was accurate only to within 3%. The thermal-conductivity ratio was more clearly defined with a probable error of less than 0.5% associated at each point below 30°K. The single error bar shown at 40°K, therefore, holds equally well for the entire curve, with the possible exception of points above 60°K, where the probable error for each measured value is around 1%.

The salient point about the anisotropies is that a_E differs from a_T , and in particular that a_E is much larger at intermediate temperatures. We may picture the anisotropy to arise from two causes: the anisotropy in the density of high-mobility electron states contributing to the conduction processes and the further anisotropy in the electron relaxation times. The former is the same for electrical and thermal conductivity, the latter can lead to differences between a_E and a_T .

In the residual-resistance region, where the Wiedemann-Franz law is obeyed, the relaxation times for electrical and thermal conduction are equal,²¹ and these conductivities therefore have the same anisotropy. The fact that a_E and a_T are equal at lowest temperatures is thus readily explained. In this regime the electrical resistivity is pictured as due to large-angle elastic scattering of electrons by impurities and defects.

Although our measurements do not extend to high temperatures, the trend of the anisotropy curves suggests that a_E and a_T become again equal above about 200°K. At these high temperatures scattering is again elastic and through large angles, and the Wiedemann-Franz law is again obeyed. One would thus expect a_E to equal a_T . The high-temperature limit of a_E or a_T would equal the value of a_E at 4.2°K if the mean angle of scattering by thermal vibrations at high temperatures were to equal the mean scattering angle for defect scattering. This is unlikely to be the case, hence the high- and low-temperature limits of the anisotropy should be different. However, both scattering processes favor large angles, so that the difference should not be large. This is borne out by the behavior of a_T .

At intermediate temperatures the Wiedemann-Franz law breaks down, indicating that the relaxation times for electrical and thermal conductivity differ. Under these circumstances a_E can be different from a_T , as is indeed the case.

At these temperatures the ideal resistivity dominates, and the electron relaxation time is governed by electron-phonon interactions. The relaxation times for electrical and thermal conduction can be related as follows²¹:

$$1/\tau_E = (1/\tau_T)(\gamma/N). \quad (7)$$

Here τ_E is the electron relaxation time for electrical conduction, τ_T is the relaxation time for thermal

conduction, γ is a numerical coefficient of order unity which should be isotropic, and N is defined below. At low temperatures the electron-phonon interaction causes the electrons to be scattered inelastically through small angles. The factor N denotes the average number of steps an electron must take in order to move in a random walk on the Fermi surface either to a zone boundary or to a region normal to the field direction.

The anisotropy in relaxation time arises mainly from the anisotropy in N . The Fermi surface of tin can be regarded as composed of segments of the free-electron Fermi sphere, bounded by the intersection of the sphere with zone boundaries. The bigger an individual segment, the larger will be N , the average number of steps a diffusing electron needs to reach a zone boundary. As different segments are weighted differently for various directions of conduction, a difference in N for different segments can lead to an anisotropy in τ_E even though there is very little anisotropy in τ_T . It is proposed here that the difference between a_E and a_T which has been observed is to be ascribed to an additional anisotropy factor for τ_E , arising from differences in N due to differences in the size of segments of the Fermi surface.

According to a model proposed by Klemens *et al.*²³ for tin, the major contribution to the conductivities comes from two types of segments on the Fermi surface: a smaller segment around the c axis, and a set of larger segments grouped about the a axes. The effective value of N should thus be larger for a -axis conduction (perpendicular orientation) than for c -axis conduction (parallel orientation), i. e., we would indeed expect a_E to exceed a_T in the temperature regime where the electron-phonon interaction is dominant but scatters electrons through small angles only.

We can attempt to draw quantitative conclusions from this model. In the limit when the length of a single step of an electron moving on the Fermi surface is small compared to the dimensions of the segment, we would expect the average number of steps N for each segment to be proportional to its area. In the model of Klemens *et al.*, where the segments are bounded by zone boundaries of non-zero structure factor, the segment areas are in the ratio 1.26 to 1. We would expect

$$a_E = a_T \frac{a\text{-axis-segment area}}{c\text{-axis-segment area}}. \quad (8)$$

Since $a_T = 1.67$, we would expect a_E to be 2.10 in the limit of low temperatures, provided it is not reduced by the residual resistivity, which becomes dominant at the very lowest temperatures. The value 2.10 should thus be a limiting value of a_E for very pure specimens. In the present case the max-

imum value of a_E was found to be 2.11, very near the estimated limit, and in reasonable agreement with it if one considers experimental uncertainties.

There is still a small anisotropy in τ_T , which causes the shallow maximum in a_T around 10°K. This is probably due to an anisotropy in the electron-phonon interaction constant and an anisotropy in the phonon spectrum. No treatment of this effect is attempted here.

ACKNOWLEDGMENTS

Three of us (M. C. K., P. G. K., and F. P. L.) acknowledge the guidance and leadership provided by Professor C. A. Reynolds, who died soon after this work was completed. The authors are indebted to H. Taylor for providing cryogenic liquids, and to Ms. L. C. Harrington, Dr. T. K. Chu, D. Strom, and M. Simard for technical assistance.

†Presented as partial requirement for the Ph. D. degree of Michael C. Karamargin, whose work was performed under the Long Term Education and Training Program of the U. S. Navy. The work was also partially supported by the U. S. Army Research Office, Durham and The University of Connecticut Research Foundation. Helium used was supplied by the Office of Naval Research.

*Present address: Naval Underwater Systems Center, New London, Conn. 06320.

‡Deceased.

¹C. A. Swenson and R. H. Stahl, *Rev. Sci. Instr.* **25**, 608 (1954).

²S. K. Case and J. E. Gueths, *Phys. Rev. B* **2**, 3843 (1970).

³B. N. Aleksandrov and I. G. D' Yakov, *Zh. Eksperim. i Teor. Fiz.* **43**, 852 (1962) [*Sov. Phys. JETP* **16**, 603 (1963)].

⁴P. W. Bridgeman, *Proc. Am. Acad. Arts Sci.* **60**, 305 (1925).

⁵J. E. Gueths, F. V. Burckbuchler, and C. A. Reynolds, *Rev. Sci. Instr.* **40**, 1344 (1969).

⁶J. E. Gueths, C. A. Reynolds, and M. A. Mitchell, *Phys. Rev.* **150**, 346 (1966).

⁷G. J. Pearson, C. W. Ulbrich, J. E. Gueths, M. A. Mitchell, and C. A. Reynolds, *Phys. Rev.* **154**, 329 (1967).

⁸J. E. Gueths, N. N. Clark, D. Markowitz, F. V. Burckbuchler, and C. A. Reynolds, *Phys. Rev.* **163**, 364 (1967).

⁹H. M. Rosenberg, *Phil. Trans.* **A247**, 441 (1955).

¹⁰C. H. Lees, *Phil. Trans. Roy. Soc. (London)* **A208**, 381 (1908).

¹¹H. M. Rosenberg, *Phil. Mag.* **2**, 541 (1957).

¹²N. V. Zavaritskii, *Zh. Eksperim. i Teor. Fiz.* **39**, 1571 (1960) [*Sov. Phys. JETP* **12**, 1093 (1961)].

¹³A. M. Guenault, *Proc. Roy. Soc. (London)* **A262**, 420 (1961).

¹⁴G. K. White and S. B. Woods, *Phil. Trans.* **A252**, 273 (1959).

¹⁵R. Bogaard and A. N. Gerritsen, *Phys. Rev. B* **3**, 1808 (1971).

¹⁶R. J. Corruccini and J. J. Gniewek, *Natl. Bur. Std. (U. S.) Monograph No. 21* (1960).

¹⁷T. Wolfram, G. W. Lehman, and R. E. Dewames, *Phys. Rev.* **129**, 2483 (1963).

¹⁸L. A. Hall, *Natl. Bur. Std. (U. S.) Tech. Note No. 365* (1968).

¹⁹F. V. Burckbuchler and C. A. Reynolds, *Phys. Rev.* **175**, 550 (1968).

²⁰V. B. Zernov and Yu V. Sharvin, *Zh. Eksperim. i Teor. Fiz.* **36**, 1038 (1959) [*Sov. Phys. JETP* **9**, 737 (1959)].

²¹P. G. Klemens, in *Thermal Conductivity*, edited by R. P. Tye (Academic, New York, 1969); also in *Handbuch der Physik*, edited by S. Flügge (Springer-Verlag, Berlin, 1956), Vol. 14.

²²E. Grüneisen and E. Goens, *Z. Physik* **26**, 250 (1924).

²³P. G. Klemens, C. van Baarle, and F. W. Gorter, *Physica* **30**, 1470 (1964).

Static Screening by a Bounded Electron Gas*

Joseph Rudnick†

Department of Physics, University of California, San Diego, California 92037

(Received 20 August 1971)

The screening of a static charge distribution inside and near the surface of a bounded quantum-degenerate electron gas is calculated in the self-consistent Hartree approximation. Special attention is paid to the Friedel-type oscillations of the screening charge density. Going inside the gas from an impurity near the surface, the oscillations are found to be larger than the corresponding oscillations in a homogeneous electron gas. The enhancement is caused by contributions to the oscillations due to electrons forward scattered by the screened potential.

I. INTRODUCTION

Quantum-mechanical screening of a static charge density near the bounding surface of a degenerate

electron gas has been discussed by several workers.¹⁻⁶ Three papers, in which the boundary of the electron gas is a plane and the bounding potential an infinite step, have been especially successful.